



Assessment of the performance of the mechatronic electrohydraulic library in a case study

Deliverable 6.2

1 Document scope

Aim of the present document is to present a strategy for the analysis and simulation of DDV electrohydraulic actuators, employed in fly-by-wire helicopters, using object-oriented techniques. A complete, detailed, DDV hydraulic servoactuator model assembled using the Modelica library for mechatronic electrohydraulic systems, presented in Deliverable 6.1, is described and a simple procedure for its integration into an existing helicopter flight mechanics model is discussed. Simulated flight tests show the practical use of the proposed approach.

2 Assessment of performance for the isolated servo

Using the basic components of the proposed library and following the architectural and mathematical model briefly described in Deliverable 6.1, the complete model of an existing prototype of a position-controlled DDV servo actuator for fly-by-wire applications was implemented and deeply tested. This actuator is designed to be supplied by two independent high-pressure (4000psi) hydraulic lines. The proportional valve, having a duplex hydraulic configuration and providing jam bypass features [26], may supply a maximum flow rate of about 7.5 l/min per hydraulic line; the nonlinear characteristics of the valve are represented in Fig.1 in terms of leakage flow and pressure sensitivity. The two lapping distances ε_S and ε_R (assuming a four-way symmetric valve $\varepsilon_{iS} = \varepsilon_S$ and $\varepsilon_{iR} = \varepsilon_R$, $i = 1, 2$) and the spool radial clearance C_r , whose real values were not known with precision, were tuned according to typical value for these parameters and in order to have approximately a leakage flow of about 1-2% of Q_{max} . The hydraulic cylinder, characterized by a dual-tandem configuration, was resized in order to comply with the indicative static requirements for the main rotor swash-plate control of a mid-weight size helicopter; the static characteristic of the actuator for both hydraulic systems operative and only one line operative is shown in Fig.2.

The spool is driven by a quadruplex torque motor (saturation current: about 2A per coil), hence four electrical armature circuits and relative 1Khz current loops were implemented; the redundant motor and driver should be connected to the helicopter DC bus, so a 28V voltage limit was assumed. Moreover, quadruplex LVDTs for the spool and ram position are present in the implemented model; hence, very different failures may be injected into the system in order to test its survivability and altered performances. The whole actuator body is mechanically joined to the airframe, but the compliance is not negligible in practice, therefore a spring-damper element was connected between the body of the actuator and the mechanical "ground" (for servo loop design, helicopter accelerations are usually neglected). The servomechanism is controlled with a cascade regulator structure closing first an inner valve loop with a PID-ISA controller (80 Hz bandwidth), which acts (at least at low

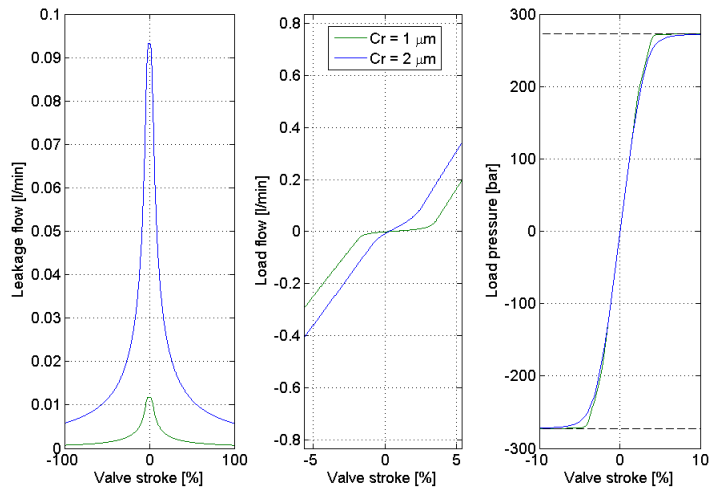


Figure 1: Leakage flow, flow gain and pressure sensitivity of the proportional valve

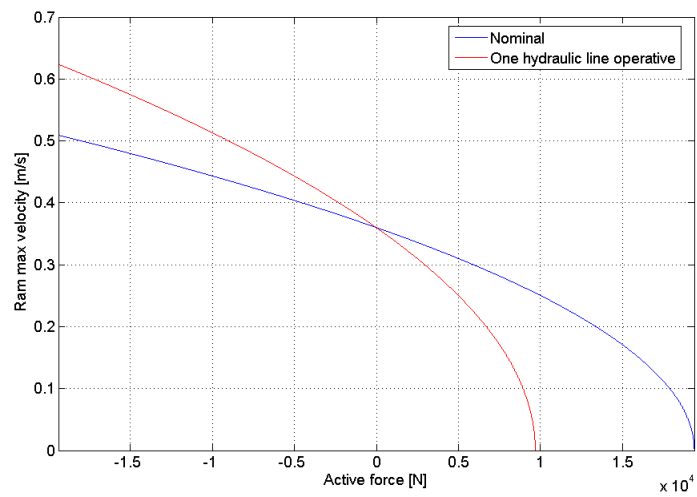


Figure 2: Actuator static characteristic

frequency) approximately as a velocity loop, and then an outer position loop for the ram, using a two-way PI compensator. The effective resulting bandwidth was esteemed exciting the input \bar{x}_p of the nonlinear model (for no load applied) with a frequency sweep having a small amplitude of 1mm and 5mm (respectively 2% and 10% of the total stroke) and performing an identification with an ARX model (Matlab function `ident`). We obtained a unitary frequency response of 8Hz at 45 deg phase lag in both cases. The frequency responses of the servo actuator are reported in Fig.3, showing the comparison with a typical nominal performance boundary for this class of systems.

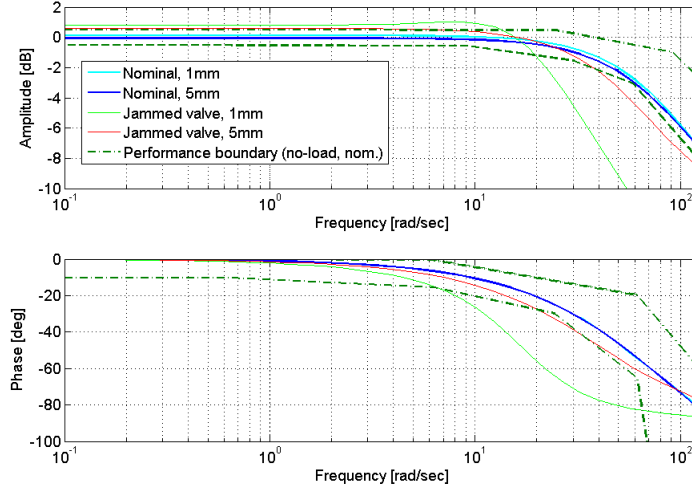


Figure 3: Actuator frequency response

From this diagram it is also apparent that the off-design jam condition is characterized by a significant performance reduction, which is very dependent on the operating amplitude, in contrast with the nominal case: we esteemed a bandwidth of about 6Hz for the 5mm case and surprisingly only 3.5Hz for the smallest amplitude case (1mm range). While the performance decrease accomplishing a jamming condition is of course related to the significant reduction of spool loop gain caused by the reaction of the detent springs, as underlined in [26], the aforementioned nonlinear behaviour cannot be predicted without a detailed mathematical model of the servomechanism.

3 The Modelica helicopter flight mechanics model

The natural step subsequent to isolated servo analysis is the integration of the actuator model into a sufficiently realistic operative scenario: this framework is represented by an existing helicopter flight mechanics simulator developed in language Modelica [7]. This rotorcraft model was developed according to the modeling paradigms defined in Padfield's book [17] for Level 1 simulators, which means helicopter flight mechanics model sufficiently detailed to predict handling qualities trends and to represent an analysis tool for the design of common mid-low bandwidth flight control systems. The interested reader is referred to [7] for a detailed discussion about the considered helicopter model; here, we just want to remember the most important features of the simulator:

- Analytical MBC (*Multi-Blade Coordinate*) main rotor model: it provides flapping states (coning, advancing and regressing modes) and rotational degree of freedom. It adopts an incompressible 2D aerodynamic model for the analytical integration of blade load. Exploiting the centre-spring equivalent rotor theory, very different blade flap retention arrangements can be reproduced (teetering, articulated and hingeless rotor).

- Main rotor inflow is reproduced with a classical three-state dynamic Pitt-Peters model [18], corrected with maneuvering distortion effects [19] which helps to improve the prediction of off-axis rotor response. The thrust generation mechanism of tail rotor, on the other hand, being characterized by much faster dynamics than main rotor, is described with a simple static inflow model based on momentum theory.
- The helicopter drivetrain dynamics is included in the model in the form of a first-order response for turboshaft engines and a PID controller representing RPM governor; a gearbox module performs the balance of mechanical power adsorbed at main and tail rotor shafts.
- The aerodynamics of lifting surfaces and fuselage is reproduced using experimental aerodynamic coefficients interpolated by means of look-up tables; simplified interaction models with main and tail rotor wakes are considered.
- The atmospheric environment is described using a standard U.S. atmosphere model for what concerns thermophysical properties, and atmospheric disturbances such as constant winds and a turbulence stochastic model (based on Dryden’s spectrum [9]) are included in the model of the environment.
- 3D terrain description can be imported (e.g. from satellite elevation data) in the simulator not only for visualization purposes, but also for simulation of IGE/OGE conditions or for the analysis of terrain-following navigation algorithms.

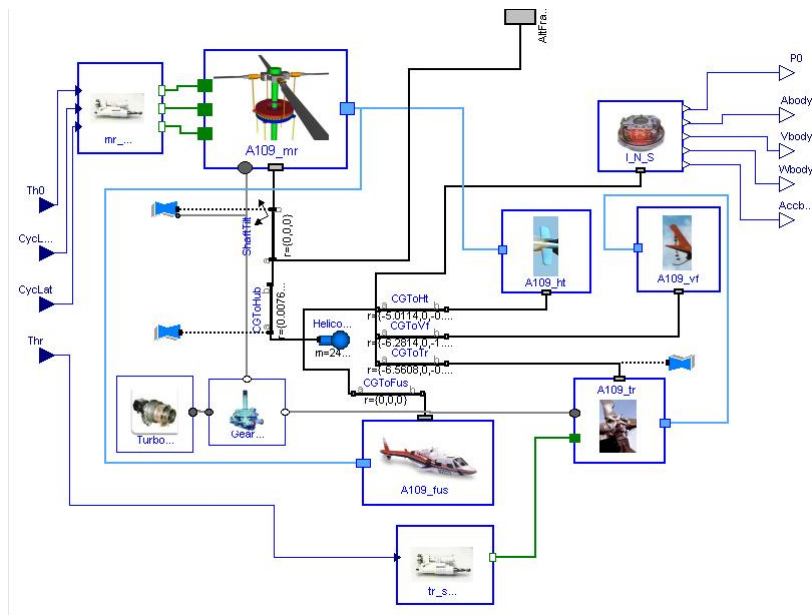


Figure 4: The Modelica helicopter simulator

Though fully parametrized, the helicopter model has been specialized recurring to the constructive and performance data of a four-bladed Agusta A109-A mkII helicopter, equipped with two Allison 250-C20B 420 shp turboshaft engines [14],[23].

Before proceeding with the description of the software integration of the electrohydraulic actuator model within the helicopter simulator, it’s worth noting that, though the flight mechanics model is not suited for predicting the aeromechanical loads acting on each stationary actuator ¹, nevertheless it can

¹as a matter of fact, we are using a common actuator disc model in which any residual periodic term, at non rotating frame, has been removed from main rotor dynamics. This fact, added to the simplifications used in the aerodynamic and mechanical description of each individual blade, does not allow an accurate recovery of the loads at rotating frame, and thus of real vibratory and unsteady loads acting on control system.

be a valuable tool for verifying whether substantial static and vibratory load levels (up to actuator's stall load), and possible faults may corrupt the closed-loop behaviour of the aircraft.

4 Integration of the servoactuator model

On a conventional single main-rotor helicopter, four main stationary servoactuators are present: three servos are used to command blade pitch of main rotor, while one servo is exploited for the control of tail rotor. It's clear that hard failures at boost servos level cannot be accepted, since the lost of one of these actuators is equivalent to a catastrophic event at helicopter level. This is the reason why boost servos are designed in order to provide *fail-operative* characteristics, exploiting physical and analytical redundancies [15]. Performance and safety requirements for swash-plate power actuators may be found in MIL-9490 specifications [1]. The linear displacement of the rod of each servoactuator, at non-rotating frame, is transformed into an equivalent blade pitch variation at the rotating frame, through swash-plate and mechanical linkages. It's worth noting that in a conventional mechanical control system the main rotor upper control system is mechanically designed (*primary mixer*) so that each actuator controls a corresponding collective or cyclic blade angle, thus one actuator governs the collective blade angle θ_0 , another the lateral blade angle θ_{1c} , and the other the longitudinal cyclic pitch θ_{1s} . Hence, each of the actuator displacement to blade pitch relationships are fully decoupled from one another. On the contrary, a modern full authority, fly-by-wire, AFCS does not present mechanical decoupling devices and the decoupling task is performed at software level. This approach greatly simplifies the helicopter, reducing weights, and it allows the so-called swash-plate reconfiguration, in order to accommodate (at least theoretically) any single actuator failure [22]. Main rotor boost actuators are usually installed with a symmetric configuration (e.g., in RAH-66 Comanche helicopter the MR servos are placed 120 degrees apart), with the fore-aft servo not necessarily located on the helicopter x -body axis; in fly-by-wire architectures, in fact, such arrangement could help possible reconfiguration strategies [22]. In the present work, we will not consider any analytical reconfiguration scheme, since the physical redundancies at actuator level exclude *a-priori* the possibility that one actuator may become stuck. For that reason, the typical geometry, depicted in Fig.5, for the main rotor actuators is assumed.

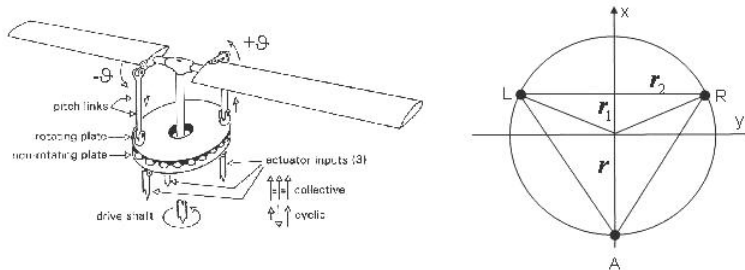


Figure 5: The control geometry of main rotor

The geometric transformation between L,A,R,T actuators (Left,Aft,Right,Tail) and main/tail rotor blade commands (Collective,Pitch,Roll,Yaw) is provided observing that the swash-plate orientation, given by the small tilt angles (ϕ_s, θ_s) , is directly related to cyclic blade angles θ_{1s} and θ_{1c} via:

$$\theta_{1s} = \theta_s \quad (1)$$

$$\theta_{1c} = -\phi_s \quad (2)$$

while a pitch link between the upper plate of the swash-plate and the blade relates the vertical displacement of the swash-plate to the collective blade pitch, so that:

$$\theta_0 = z_s/l_{mr} \quad (3)$$

The total main-rotor blade pitch can be expressed as a function of the blade azimuthal position ψ with the well-known relation:

$$\theta(\psi) = \theta_0 + \theta_{1c} \cos(\psi) + \theta_{1s} \sin(\psi) \quad (4)$$

Tail rotor collective pitch is varied according to a relation analogous to (3). Under small angle approximation, swash-plate tilt can be easily related to the displacements of each main rotor actuator rod:

$$\begin{bmatrix} \Delta_L \\ \Delta_R \\ \Delta_A \end{bmatrix} = \begin{bmatrix} 1 & r_1 & r_2 \\ 1 & r_1 & -r_2 \\ 1 & -r & 0 \end{bmatrix} \begin{bmatrix} z_s \\ \theta_s \\ \phi_s \end{bmatrix} \quad (5)$$

Considering the equations (1),(3) and (5) the complete expression for the control mixing can be derived:

$$\begin{bmatrix} \Delta_L \\ \Delta_R \\ \Delta_A \\ \Delta_T \end{bmatrix} = \begin{bmatrix} l_{mr} & r_1 & -r_2 & 0 \\ l_{mr} & r_1 & r_2 & 0 \\ l_{mr} & -r & 0 & 0 \\ 0 & 0 & 0 & l_{tr} \end{bmatrix} \begin{bmatrix} \theta_0 \\ \theta_{1s} \\ \theta_{1c} \\ \theta_{tr} \end{bmatrix} \quad (6)$$

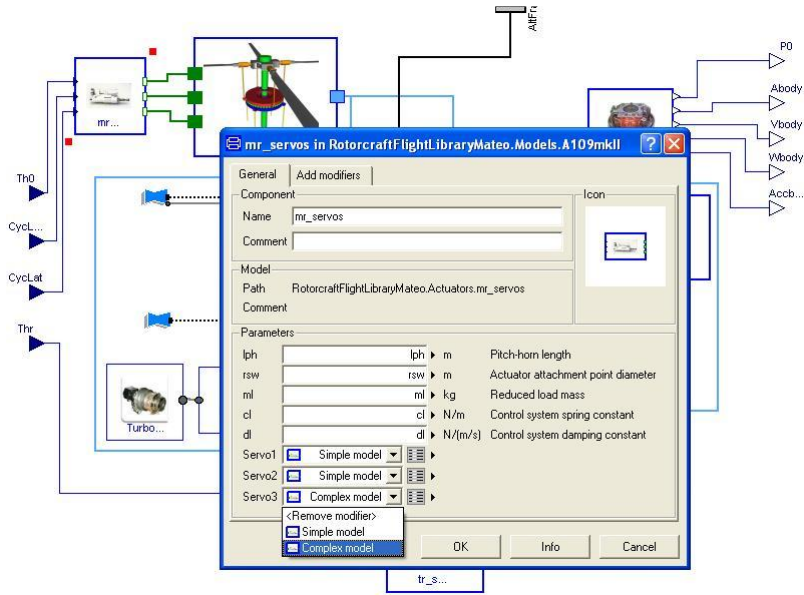


Figure 6: Choice of actuator level of detail

The dynamic behaviour of each servoactuator can of course be reproduced with growing level of detail; the simplest model is represented by a second order dynamical system with a saturation and a rate limiter block: this is the model commonly adopted in the context of flight simulation and control system analysis and it's suitable for the prediction of the response of servoactuators in nominal conditions. The produced library allows the final user to easily select also higher level of detail (Fig. 6), among which a medium-level model providing a detailed (but simplex) hydraulic system

and no electrical dynamics, and the detailed redundant DDV model described in the Deliverable 6.1 and used for the performance assessment of the isolated servo. The choice depends on the required trade-off between accepted computational burden (e.g. simplified current loops, that is without the model of PWM, need at least 0.1-0.5 msec for the integration timestep) and the desired accuracy, since nonlinear effects and dynamical couplings play an important role in this class of systems. Full detail actuator models allow not only more realistic results, but provide also a practical instrument for simulating failure conditions. The integration of the servoactuator model, developed with the Modelica mechatronic electrohydraulic library, has been made possible implementing two actuator modules, one for main rotor (assembly of three servoactuators, Fig.7) and one for tail rotor. Each module provides the required geometric transformations (i.e. eq. (6)), the simplified model (1 dof) of the mechanical impedance attached to the rod (but more complex models can be of course be reproduced, if available) and the Modelica records, reporting technical data, used for the parametrization of the whole module. Mechanical flanges, extracted from `Translational` subpackage of `Modelica.Mechanics` library, are used to physically connect each module to the correspondent flight mechanics subsystem (e.g. main rotor class).

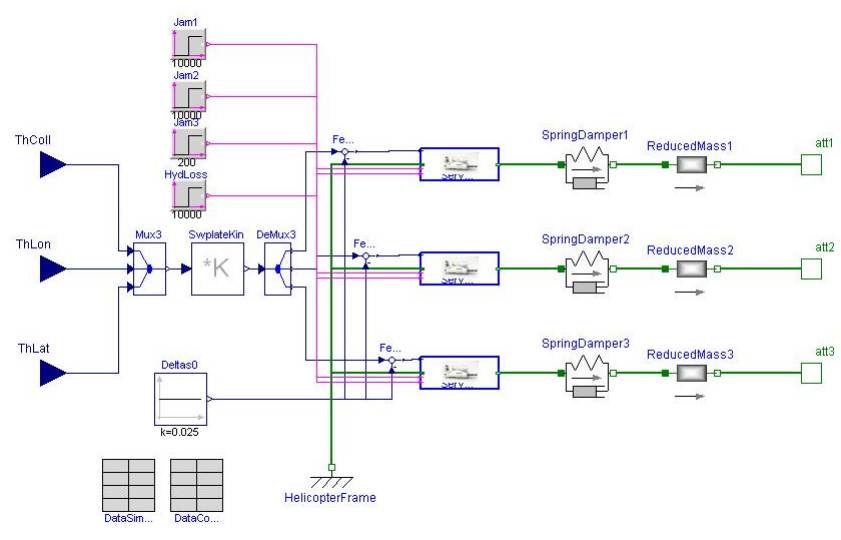


Figure 7: Main rotor servos assembly

5 The fly-by-wire AFCS model

Different full-authority AFCS (Automatic Flight Control Systems) architectural and design solutions for fly-by-wire rotorcrafts can be found in literature; nevertheless, many of these solutions share a common inner-outer loop structure. Thus, the AFCS architecture adopted for our analyses is an inner-outer loop scheme with the following characteristics:

- Inner loops: ACAH (Attitude Command, Attitude Hold)
- Outer loops: hold modes (IAS hold, HDG hold, ALT hold) and automatic turn coordination

Digital flight control laws have been implemented with a standard 50Hz update frequency; the inner loop cyclic outputs, before software de-mixing in the main rotor actuators module, undergoes a further transformation needed to apply a shifted phase angle in rotor flapping response to cyclic commands (instead of the theoretical 90 deg). The ACAH control laws provided by the inner loops have been designed according to a Linear Quadratic explicit model following technique, called also CGT (*Command Generator Technique*) [6],[12]. This strategy adds the flexibility and robustness

of the LQR control with the attractive features of model following control, which are particularly desired in aeronautical applications, where closed-loop dynamic performances are often prescribed by regulations. Let's consider the 8-th order linearized helicopter plant model (obtained with order reduction techniques or with identification methods) and the reference model described, in state space, by:

$$\begin{bmatrix} \dot{x} \\ \dot{x}_m \end{bmatrix} = \begin{bmatrix} A & 0 \\ 0 & A_m \end{bmatrix} + \begin{bmatrix} B \\ 0 \end{bmatrix} u + \begin{bmatrix} 0 \\ B_m \end{bmatrix} r \quad (7)$$

where $r = [r_\phi, r_\theta, r_w, r_r]'$ represents a vector of commands (respectively, roll attitude command, pitch attitude command, heave velocity command and yaw rate command) and the performance vector $z = [\phi, \theta, w, r]'$ simply select the variables of the tracking problem (roll, pitch, heave velocity and yaw rate) from the state vector $x = [\phi, \theta, u, v, w, p, q, r]'$; the control input vector is $u = [\theta_0, \theta_{1c}, \theta_{1s}, \theta_{tr}]$. For sake of brevity, let's rewrite the systems (7) (plant plus model) in the compact form:

$$\dot{\tilde{x}} = \tilde{A}\tilde{x} + Bu + Gr, \quad \tilde{x} \in \mathcal{R}^{16 \times 1} \quad (8)$$

The command generator technique assumes that, for some initial conditions, the reference command satisfies the differential equation

$$r^d + a_1 r^{d-1} + \dots + a_d r = 0 \quad (9)$$

or, in polynomial form, $\Delta(s)r = 0$. Substituting (9) in the system (8) the auxiliary model

$$\dot{\xi} = \tilde{A}\xi + \tilde{B}\mu \quad (10)$$

with $\xi = \Delta(s)\tilde{x}$ and $\mu = \Delta(s)u$ can be obtained. In the special case of step commands, useful for ACAH design, we simply have $d = 1$, $a_1 = 0$ hence $\xi = \dot{\tilde{x}}$ and $\mu = \dot{u}$. Considering $H_m = H$ the tracking error $e = Hx_m - Hx$ satisfies:

$$\dot{e} = \Delta(s)e = [-H, H]\xi = \tilde{H}[\xi'_p, \xi'_m]' \quad (11)$$

which allows to consider the augmented system:

$$\begin{bmatrix} \dot{e} \\ \dot{\xi} \end{bmatrix} = \begin{bmatrix} 0 & \tilde{H} \\ 0 & \tilde{A} \end{bmatrix} \begin{bmatrix} e \\ \xi \end{bmatrix} + \begin{bmatrix} 0 \\ B \end{bmatrix} \mu \quad (12)$$

$$\dot{\hat{\xi}} = \hat{A}\hat{\xi} + \hat{B}\mu, \quad \hat{\xi} = [e', \xi']' \quad (13)$$

The LQ regulator design can be executed considering the infinite-horizon performance index:

$$J = \frac{1}{2} \int_0^\infty e' Q e + \mu' R \mu dt = \frac{1}{2} \int_0^\infty \hat{\xi}' \tilde{Q} \hat{\xi} + \mu' R \mu dt \quad (14)$$

having set $\tilde{Q} = C'_e Q C_e$ and $C_e = [I_4, 0_{4 \times 16}]$. It's worth nothing that, differently from standard LQR designs, in this case weight matrices can be easily assigned: $Q = I_4$, $R = \rho I_4$. The optimal control law expresses a state-feedback in the form:

$$\mu_o = \tilde{K}\hat{\xi} = [K_e \quad K_p \quad K_m] \begin{bmatrix} e \\ \xi_p \\ \xi_m \end{bmatrix} \quad (15)$$

which can be written also as:

$$u_o(t) = K_e \int_0^t e(\tau) d\tau + K_p x(t) + K_m x_m(t) \quad (16)$$

The control law given by (16) requires measurement or real-time estimation of the entire flight mechanics state vector; if we exclude side velocity v , which needs to be estimated in practice using an observer or a Kalman filter since this air-data quantity is much noisy due to rotor environment, and the heave velocity w , which is not directly measured and should be reconstructed from other measurements, the other states are commonly measured on modern helicopters: attitudes and rates measurements are extracted from the helicopter strapdown AHRS with a good accuracy and low noise to signal ratio, while airspeed u is extracted from air data computer. In our study, the fundamental nonlinearities of the plant, which arise with the variation of advance ratio, are compensated for scheduling the three gain matrices with IAS: $K_e(u), K_p(u), K_m(u)$. No scheduling with altitude has been provided for our tests, though important in practical implementations, since the effect of density variation plays an important role only for significative height excursions. The linear models used for control design have been extracted from the full nonlinear model, trimming the helicopter model in forward flight at different airspeeds; the resulting high-order models have been order reduced residualizing the fast dynamics (or less involved with flight mechanics), such as main rotor, inflow and engine dynamics. Expression (16) shows also that a reference model for tracking should be run together with flight control laws; the adopted linear model, derived from [12], specifies a first-order response for heave and yaw channel and a second-order response for roll and pitch:

$$\begin{aligned} \dot{\phi} &= p \\ \dot{\theta} &= q \\ \dot{u} &= -\lambda_u u - \lambda_u \theta \\ \dot{v} &= -\lambda_v v + \lambda_v \phi \\ \dot{w} &= -\lambda_w w + \lambda_w r_w \\ \dot{p} &= -2\xi_\phi \omega_\phi p - \omega_\phi^2 \phi - \omega_\phi^2 r_\phi \\ \dot{q} &= -2\xi_\theta \omega_\theta q - \omega_\theta^2 \theta - \omega_\theta^2 r_\theta \\ \dot{r} &= -\lambda_r r + \lambda_r r_r \end{aligned} \quad (17)$$

The LTI model (17) has been tuned in order to achieve, according to ADS-33 specifications [2] for Level 1 and 2 handling qualities performances, a nominal bandwidth of 3 rad/sec for pitch, 3.5 rad/sec for roll, 2 rad/sec for heave and 3.5 rad/sec for yaw, and a value of 0.7 for pitch and roll damping.² The outer loops are implemented using standard PI controllers and filters and they provide, as said before, hold modes (airspeed, altitude and heading) and an automatic turn coordination function; with the aid of integral states, these regulators guarantees the robust automatic trim of the helicopter for different flight conditions, in the entire flight envelope.

6 Case study

For the simulation studies discussed in this deliverable, the mechanical properties of each servoactuator ground attachment and load impedance have been tuned according to typical specification documents for helicopter boost servos of the same category. The external load acting on servos has been simulated with an empirical spectrum characterized by a DC component plus a n_b/rev vibratory load (about

²It's common practice in helicopter community to design basic stabilization laws with slightly lower performance than the maximum possible, in order to avoid dynamic coupling with rotor dynamics and to satisfy the pilots' requests, who often find Level1 HQ performances to much aggressive for a smooth ride.

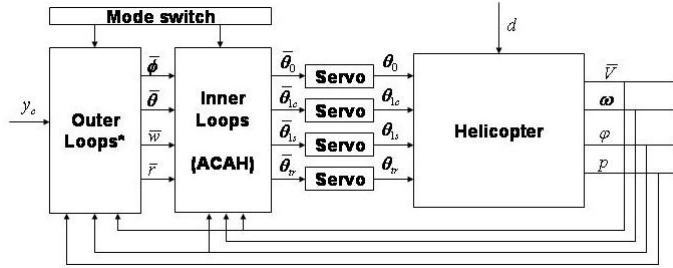


Figure 8: General structure for a full authority AFCS

25Hz for the four-bladed 380rpm main rotor of the A109), as suggested in specialized literature. The amplitude of external loads has been set according to two different load scenarios:

- Load case 1: load peak amplitude 98% of stall load (for two hydraulic lines operative), 62%DC plus 36% vibratory.
- Load case 2: 50% of Load case 1.

The empirical characterization of external loads is justified, in practice, by the difficult airload predictability with affordable mathematical models and the quite good disturbance rejection of the servoactuator at all frequencies. Detailed aeroelastic models for the load can of course improve the accuracy of the simulation, but requiring typically much more computational power and development time [21]. A thorough description of numerical methods useful for helicopter flight control system analysis, in case of traditional power actuators with mechanical feedback, is given in [16].

In order to increase control activity during the simulated flight transients, atmospheric turbulence is activated setting the relative parameters to "severe turbulence" level [9] (horizontal intensity $\sigma_h = 5.7\text{m/sec}$, lateral and vertical intensity $\sigma_{v,w} = 4.67\text{m/sec}$, horizontal scale length $L_u=832\text{m}$ and lateral/vertical scale length $L_{v,w}=624\text{m}$). In the present document, two simulated flight tests are reported: in the first test (Fig. 9), the helicopter starts hovering then, for $t=30\text{sec}$, a fast vertical climb (1575 ft/min) is commanded to the ACAH controller. After a short yaw-rate impulse ($t=50\text{sec}$), the helicopter decreases pitch attitude gaining longitudinal velocity. In Fig.10, some significative transients of main rotor fore-aft servo for both load conditions 1 and 2 are shown. For $t=50\text{sec}$ a valve jam fault is injected into the system, as it's evident from the increase of the average level of absorbed current (the jam condition forces the motor to contrast the detent spring pre-load of 10Kgf in order to drive the inner sleeve and form the new flow path). Despite of the faulted configuration, anyway, the DDV spool jam proofness guarantees that the actuator keeps its positioning capability.

In the second test, the helicopter performs a straight flight accelerating from hover to 100kts, then ($t=120\text{sec}$) the AFCS commands a square tooth variation for roll and pitch attitudes and heave velocity. In this case the control activity is much higher than in the first test, as it's clear from Fig. 11 and from the mechanical and electrical transients of the aft servo (Fig. 12). The same fault of test 1 is injected for $t=200\text{sec}$, but this time the noisy current signal, which is almost saturated, significantly hides the fault event. As in the previous case, the actuator dual-path structure ensures a good robustness to the system, allowing it to provide good performances also in faulted conditions; for that reason, flight mechanics does not exhibit any significative performance decrease.

7 Conclusions and outlook

In this document, we have shown how to exploit the Modelica library for mechatronic electrohydraulic actuators, presented in Deliverable 6.1, for the simulation of a detailed DDV hydraulic actuator for fly-by-wire applications. The model of the isolated servomechanism has been deeply analyzed for

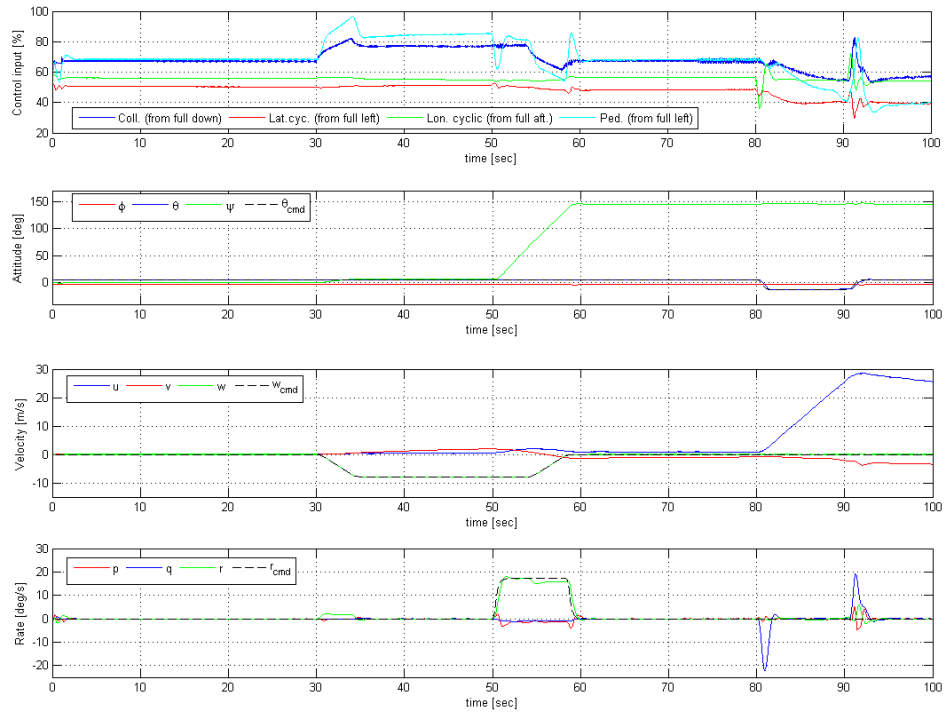


Figure 9: Flight test 1 - flight mechanics quantities

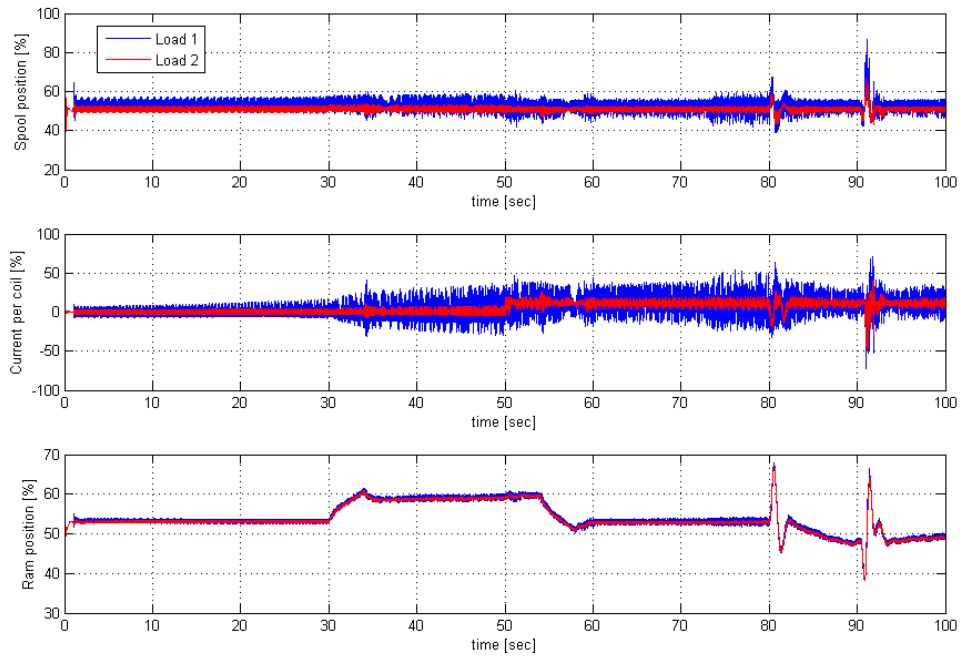


Figure 10: Flight test 1 - dynamic transient of main rotor aft servo

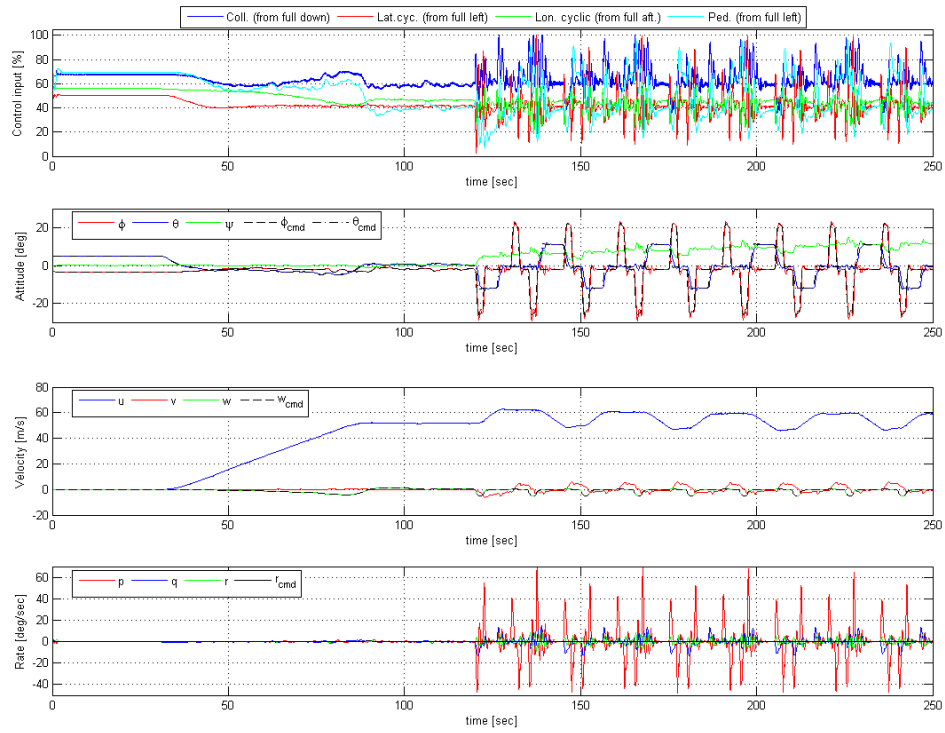


Figure 11: Flight test 2 - flight mechanics quantities

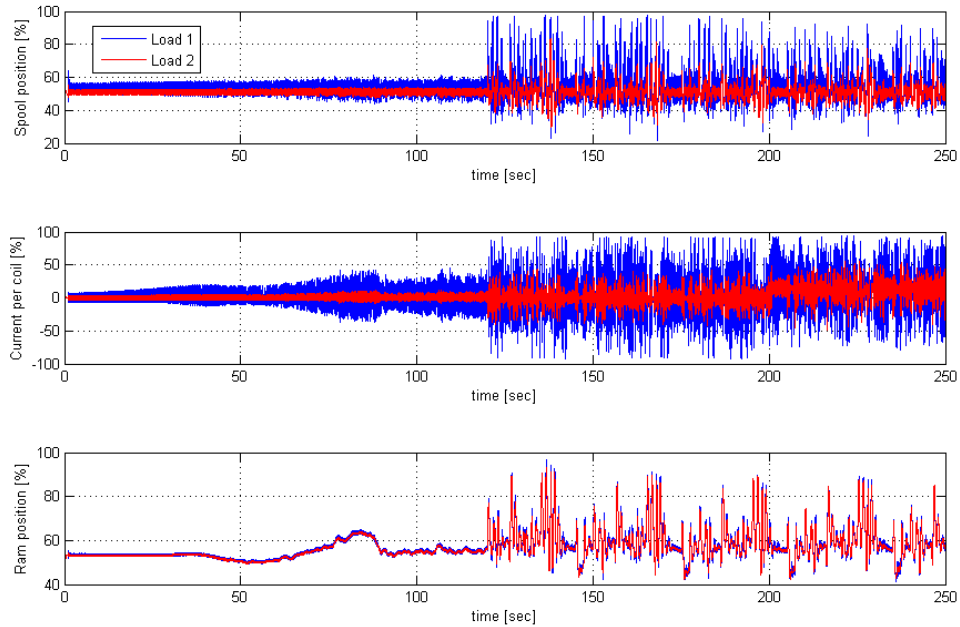


Figure 12: Flight test 2 - dynamic transient of main rotor aft servo

different operative conditions, then we have described the procedure needed to integrate this model into an existing Modelica helicopter flight mechanics model in a way to preserve modularity for both models. The resulting simulator, which is fully configurable according to user's need, allows to perform sensitivity analysis with respect to highly uncertain parameters (e.g. external load acting on stationary servos) and to facilitate the avionic integration of fly-by-wire hydraulic actuators. Sophisticated aerodynamic/aeroelastic codes (such as CAMRAD/JA) may be exploited to compute reduced-order impedance models and trim loads which can be used in the proposed model with the aim of improving simulation realism and reducing design conservatism.

References

- [1] Anonymous. General Specifications for Flight Control Systems: Design, Installation and Test of Piloted Aircraft. MIL.SPEC. MIL-F-9490D, U.S.A.F., June 1975.
- [2] Anonymous. Handling Qualities Requirements for Military Rotorcraft. MIL.SPEC. ADS-33E, U.S. Army Aviation Systems Command, February 2000.
- [3] B.H. Wilson B. Eryilmaz. A Unified Model of a Proportional Valve. In *ASME Fluid Power Systems and Technology Division*, volume FPST-6, pages 95–102.
- [4] B.H. Wilson B. Eryilmaz. Modeling the Internal Leakage of Hydraulic Servovalves. In *ASME Dynamic Systems and Control Division*, volume DSC-69.1, pages 337–343.
- [5] P. Beater. Modeling and Digital Simulation of Hydraulic Systems in Design and Engineering Education using Modelica and HyLib. In *Modelica Workshop 2000*, Lund, Sweden, 2000.
- [6] L.F. Lewis B.L. Stevens. *Aircraft control and simulation*. Wiley, New York, 1992.
- [7] L. Viganò G. Magnani. Acausal modelling of helicopter dynamics for automatic flight control applications. In *5th Modelica International Conference*, pages 377–384, Vienna, Austria, September 2006.
- [8] C. Chen J. Lin. Buck/Boost Servo Amplifier for Direct-Drive-Valve Actuation. *IEEE Transactions on Aerospace and Electronics Systems*, 31(3):960–967, 1995.
- [9] J.D.McMinn. Extension of a Kolmogorov atmospheric turbulence model for time-based simulation implementation. In *AIAA Guidance, Navigation, and Control Conference*, New Orleans, USA, August 1997.
- [10] K.R. Goheen J.K. Pieper, S.Baillie. Linear-Quadratic Optimal Model-Following Control of a Helicopter in Hover. In *American Control Conference*, Baltimore (MD), USA, June 1994.
- [11] P.Rocco L. Viganò, G. Magnani and T.Busi. An object-oriented library for mechatronic electro-hydraulic systems. In *ANIPLA Motion Control 2007 symposium*, Milan, Italy, May 2007.
- [12] J.K. Pieper M. Trentini. Model-Following Control of a Helicopter in Hover. In *IEEE International Conference on Control Applications*, Dearborn (MI), USA, September 1996.
- [13] H.E. Merritt. *Hydraulic Control Systems*. Wiley, New York, 1967.
- [14] G. Bonaita M.M. Eshow, D. Orlandi and S. Barbieri. Results of an A109 Simulation Validation and Handling Qualities Study. Technical Report USAAVSCOM 88-A-002, Aeroflightdynamics Directorate (U.S. Army Research and Tecnology Activity), Agusta SpA and Italian Air Force/D.A.S.R.S.-R.S.V. , May 1989.
- [15] S. Osder. Practical View of Redundancy Management Application and Theory. *Journal of Guidance, Control and Dynamics*, 22(1):12–21, 1999.

- [16] P.A. Nour C. Monteggia P. Masarati, P. Mantegazza and R. Raval. Helicopter Control System Synthesis by Multibody Multidisciplinary Analysis. In *European Rotorcraft Forum*, Bristol, UK, 2002.
- [17] G.D. Padfield. *Helicopter flight dynamics : the theory and application of flying qualities and simulation modelling*. Oxford : Blackwell, 1996.
- [18] D.M. Pitt and D.A. Peters. Theoretical prediction of dynamic-inflow derivatives. *Vertica*, 5(1):21–34, 1981.
- [19] F. Tchen-Fo P.M. Basset. Study of the rotor wake distortion effects on the helicopter pitch - roll cross couplings. In *24th European Rotorcraft Forum*, Marseilles, France, September 1998.
- [20] P.Y. Li Q. Yuan. Using Steady Flow Force for Unstable Valve Design: Modeling and Experiments. *Journal of Dynamic Systems, Measurement, and Control*, 127:451–462, 2005.
- [21] J.E. Duh R. Sopher. Prediction of Control System Loads in Level Flight and Maneuvers. In *American Helicopter Society 50th Annual Forum*, volume 2, pages 1303–1321, Washington DC, USA, 1994.
- [22] J.Si R.Enns. Helicopter Flight-Control Reconfiguration for Main Rotor Actuator Failures. *Journal of Guidance, Control and Dynamics*, 26(4):572–584, 2003.
- [23] R.K.Heffley and M.A.Mnich. Minimum-complexity helicopter simulation math model. Contractor report NASA 177476, Aeroflightdynamics Directorate, U.S. Army Research and Tecnology Activity (AVSCOM), April 1988.
- [24] K.Kimura S.Ozeki and T.Tomio. Flight simulation using actual helicopter equipped with full-authority FBW system. In *AIAA Modeling and Simulation Technologies Conference*, Denver (CO), USA, 2000.
- [25] W.J. Thayer. Specification standards for electrohydraulic flow control servovalves. Technical report, Moog inc., 1962.
- [26] K.Kazuo Y.Wataru and F.Tatsuru. Direct drive valve (DDV) hydraulic actuator for helicopter FBW. In *24th European Rotorcraft Forum*, Marseilles, France, 1998.